3D segmentation and classification of single trees with full waveform LIDAR data

J. Reitberger[1], P. Krzystek[1] & U. Stilla[2]

[1]Dept. of Geoinformatics, University of Applied Sciences Muenchen, 80333 Munich, Germany, josef.reitberger@hm.edu, krzystek@hm.edu
[2]Photogrammetry and Remote Sensing, Technische Universitaet Muenchen, 80290 Munich, Germany, stilla@tum.de

Abstract

The paper highlights a new 3D segmentation technique that detects single trees with an improved accuracy. The method uses the normalized cut segmentation and is combined with a special stem detection method. A subsequent classification identifies tree species using salient features that utilize the additional information the waveform decomposition extracts from the reflected laser signal. Experiments were conducted in the Bavarian Forest National Park with conventional first/last pulse data and full waveform LIDAR data. The first/last pulse data result from a flight with the Falcon II system from TopoSys in leaf-on situation at a point density of 10 points/m^2. Full waveform data were captured with the Riegl LMS Q-560 system at a point density of 25 points/m^2 (leaf-off and leaf-on) and at a point density of 10 points/m^2 (leaf-on). The study results prove that the new 3D segmentation approach is capable of detecting small trees in the lower forest layer. This was practically impossible so far if tree segmentation techniques based on the canopy height model (CHM) were applied to LIDAR data. Compared to the standard watershed segmentation the combination of the stem detection method and the normalized cut segmentation performs better by 12%. In the lower forest layers the improvement is even more than 16%. Moreover, the experiments show clearly that the usage of full waveform data is superior to first/last pulse data. The unsupervised classification of deciduous and coniferous trees is in the best case 93%. If a supervised classification is applied the accuracy is slightly increased with 95%.

Keywords: LIDAR, Analysis, Segmentation, Forestry, Vegetation

1. Introduction

Single tree detection has been a key issue in forest inventory research. So far, nearly all methods have tackled the problem to detect single trees from the CHM, which is a result of a surface interpolation. Approaches presented – for instances – by Hyyppä et al. (2001), Solberg et al. (2006) or Brandtberg (2007) stand for such kind of methods. Typically, the detection rate of single trees is limited due to unavoidable smoothing effects in the interpolated surface. The main drawback is that trees and young regeneration in the intermediate and lower forest layers are invisible from the CHM surface and hence cannot be detected at all. Tree species classification using solely LIDAR data and features derived from the coordinates of the laser returns has been investigated – for instance – by Holmgren et al. (2004) who showed that the coniferous tree species Norway spruce and Scots pine can be classified with an overall accuracy of 95% using highly dense LIDAR data. Heurich (2006) demonstrates that classification of Norway spruce and European beech is possible with an overall accuracy of 97% in leaf-off situation. However, the tree segments were derived from LIDAR data acquired in leaf-on situation. The study refers to LIDAR data with a mean point density of 10 points/m^2 and clearly shows that desirable forest features like young regeneration could not be detected.

Recent advances in LIDAR technology have generated new full waveform scanners that provide a higher spatial point density and additional information about the reflecting characteristics of trees. Important issues like the calibration and the decomposition of full waveform data with a series of Gaussians, as well as the detection and classification of vegetation have been investigated by Wagner et al. (2006), Jutzi and Stilla (2006), Kirchhof et al. (2008) and Reitberger et al. (2008a). Recently, Reitberger et al. (2008c) successfully showed that the new full waveform technology can significantly improve the detection rate of single trees using a 3D segmentation technique based on the normalized cut segmentation.

In this paper we present results of a tree species classification with full waveform data based on this new encouraging 3D tree segmentation technique. The objective of this paper is (i) to shortly highlight the new segmentation method that extracts single trees using full waveform LIDAR data, (ii) to demonstrate the improved detection rate of single trees, (iii) to prove the benefit of full waveform data both in leaf-on and leaf-off situation at different point densities, and (iv) to present classification results of a) deciduous and coniferous trees and b) spruces and fir trees.

2. Method

2.1 Normalized cut segmentation

The motivation of the normalized cut segmentation is to overcome the disadvantages of a CHM based watershed segmentation (e.g. Reitberger et al., 2008a), which calculates the tree positions $(X^{CHM}_{stem\ i}, Y^{CHM}_{stem\ i})(i = 1,...,N_{seg})$ from the local maxima of the CHM. Thus, neighbouring trees are often not separated and form a tree group instead of single trees. Moreover, smaller trees in the intermediate and lower height level cannot be recognized since they are invisible in the CHM. A special stem detection method (Reitberger et al., 2007) separates neighbouring trees and provides the stem positions $(X^{StDet}_{stem\ i}, Y^{StDet}_{stem\ i})$ $(i = 1,...,N_{StDet})$ if there are enough stem reflections, and if the stem area can be reliably separated from the crown points by the crown base height. It fails of course when young regeneration and small trees are located below tall trees. A further drawback is that the crown points belonging to the original segment are not separated with respect to the detected stems. In order to tackle these problems we have set up a true 3D segmentation of single trees using the normalized cut method known from image segmentation (Shi and Malik, 2000), which uses the positions (x_i, y_i, z_i) of the reflections and optionally the pulse width W_i and the intensity I_i of the waveform decomposition (Reitberger et al., 2008b).

This segmentation divides a graph G formed by voxels given in a region of interest (ROI) into disjoint segments A and B (Figure 1a) by maximizing the similarity of the segment members and minimizing the similarity between the segments A and B. The corresponding cost function is

$$NCut(A,B) = \frac{Cut(A,B)}{Assoc(A,V)} + \frac{Cut(A,B)}{Assoc(B,V)} \qquad (1)$$

with $Cut(A,B) = \sum_{i \varepsilon A, j \varepsilon B} w_{ij}$ as the total sum of weights between the segments A and B and $Assoc(A,V) = \sum_{i \varepsilon A, j \varepsilon V} w_{ij}$ representing the sum of the weights of all edges ending in the segment A. The weights w_{ij} between two voxels are basically a function of the LIDAR point distribution and features calculated from W_i and I_i. They define the similarity between the voxels. The minimization of *NCut(A,B)* is solved by a corresponding generalized eigenvalue problem (Reitberger et al., 2008b). The approach can use auxiliary data like, for instance, the information

about the local maxima of a CHM $(X_{stem\ i}^{CHM}, Y_{stem\ i}^{CHM})(i = 1,...,N_{seg})$ in order to weight the similarity between the voxels below the CHM maxima. Also, the results of the stem detection $(X_{stem\ i}^{StDet}, Y_{stem\ i}^{StDet})(i = 1,...,N_{StDet})$ can be introduced to provide special weights for the voxels similarity. The figure 1b shows complex situations where the normalized cut segmentation works excellent and where the watershed segmentation and the stem detection fail.

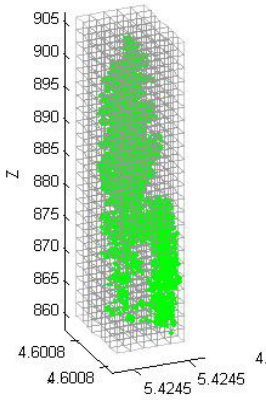

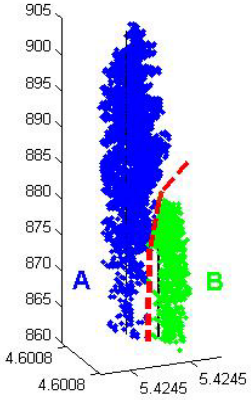

Figure 1a: Subdivision of ROI into a voxel structure and division of voxels into two tree segments A and B

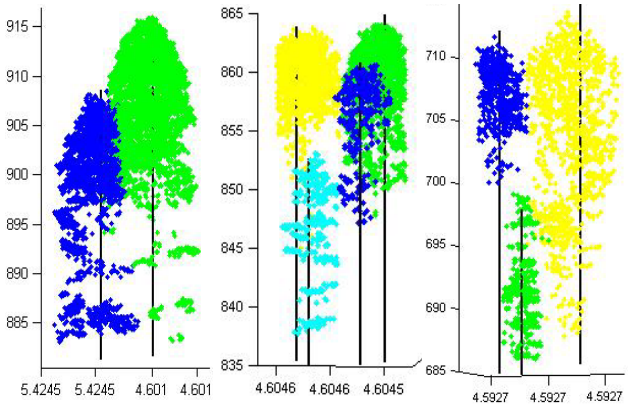

Figure 1b: Examples of normalized cut segmentation with the reference trees as black vertical lines

2.2 Classification

We consider different types of salient features $S_t = \{S_g, S_{i,}, S_I, S_W, S_n\}$ for the classification that are calculated using the N_t LIDAR points $\boldsymbol{X}_i^T = (x_i, y_i, z_i, W_i, I_i)$ $(i = 1,...,N_t)$ in the segments. They are subdivided into five groups reflecting the outer tree geometry by S_g, the internal geometrical tree structure by S_i, the intensity-related features by S_I, the pulse width characteristics by S_W, and the number of reflections per waveform by S_n. Table 1 gives a short overview of the saliency definitions (see details Reitberger et al., 2008a).

Table 1: Definition of saliencies ("Sal.") used in classification

Sal.	Definition	Sal.	Definition
S_g^1	Parameters $\{a_1,a_2\}$ of a parabolic surface	S_I^2	Mean intensity in entire tree
S_g^2	Mean distances of layer points to tree trunk	S_W	Mean pulse width of single and first reflections in the entire tree segment
S_i^h	Percentiles of the LIDAR points	S_n^1	Average number of reflections between the first and last reflection in the waveform
S_i^d	Percentage of LIDAR points in a tree height layer	S_n^2	Relation of the number of single reflections to the number of multiple reflections
S_I^1	Mean intensities of height layers		

Tree species are classified both by an unsupervised and a supervised classification. Let S_t be the salient features of a tree t to be classified and let $C_k = \{\mu_k, \Sigma_k\}$ be the density probability model (mean, covariance matrix) of the k^{th} tree class. The clusters of different tree species are found by the Expectation-Maximization algorithm that approximates the distribution of a saliency subset S ε S_t by fitting the parameters of the density model $p(S) = \sum_{k=1}^{s} \pi_k N(S \mid \mu_k, \Sigma_k)$ to

the data by a maximum-likelihood estimation with π_k as the mixing coefficients, $N(S \mid \mu_k, \Sigma_k)$ as the multivariate Gaussian distribution and *s* as the number of Gaussians (Heijden et al., 2004). The clusters of tree species statistically described by C_k are the results of the unsupervised classification. The supervised classification is a maximum likelihood classification by estimating the density probability models $C_k = \{\mu_k, \Sigma_k\}$ from a training subset S_{train} with $\hat{\mu}_k = \frac{1}{N_k}\sum_{n=1}^{N_k} S_n$ and $\hat{\Sigma}_k = \frac{1}{N_k - 1}\sum_{n=1}^{N_k}(S_n - \hat{\mu}_k)(S_n - \hat{\mu}_k)^T$ where N_k is the number of samples of the k^{th} class. The probability that a tree *t* with the saliencies S_t is a member of the k^{th} tree class is given by

$$p(S_t|C_k) = \frac{1}{(2\pi)^{\frac{d}{2}}\sqrt{\left|\hat{\Sigma}_k\right|}} \exp\left(-\frac{1}{2}(S_t - \hat{\mu}_k)^T \hat{\Sigma}_k^{-1} (S_t - \hat{\mu}_k)\right) \quad (2)$$

with *d* as the number of salient features.

3. Experiments

3.1 Material

Experiments were conducted in the Bavarian Forest National Park (49° 3' 19" N, 13° 12' 9" E) which is located in South-Eastern Germany along the border to the Czech Republic (Figure 2). There are four major test sites of size between 591 ha and 954 ha containing sub alpine spruce forest, mixed mountain forest and alluvial spruce forest as the three major forest types.

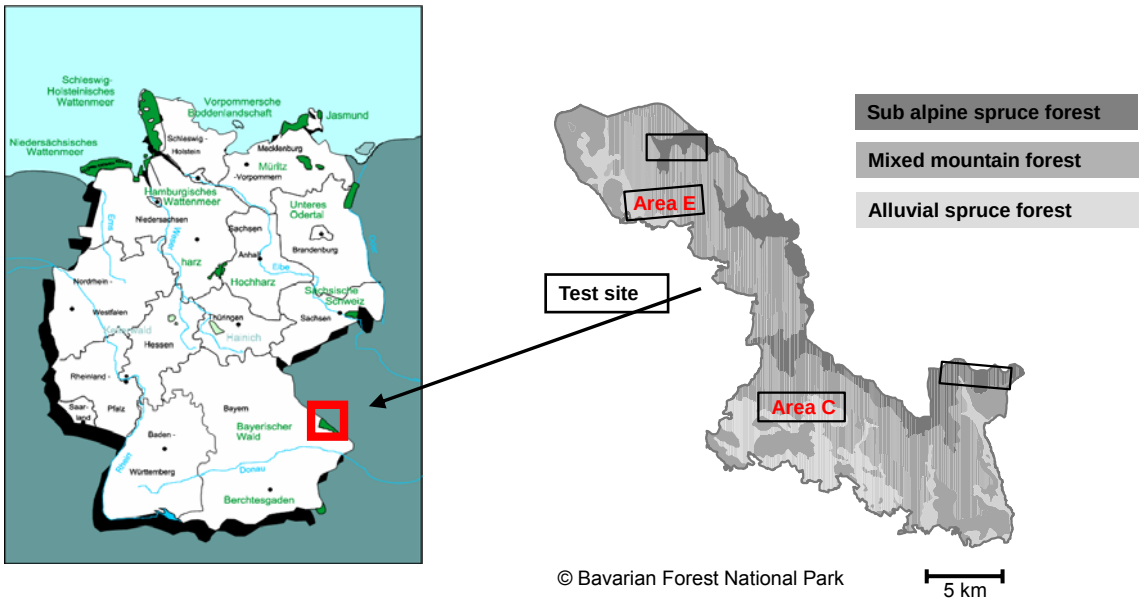

Figure 2: Location of the Bavarian Forest National Park in the map of Germany (left) and map of the park with its forest types and test sites (right).

18 sample plots with an area size between 1000 m^2 and 3600 m^2 were selected in the test sites E and C (Figure 3). Reference data for all trees with DBH larger than 10 cm have been collected for 688 Norway spruces (*Picea abies*), 812 European beeches (*Fagus sylvatica*), 70 fir trees (*Abies alba*), 71 Sycamore maples (*Acer pseudoplatanus*), 21 Norway maples (*Acer platanoides*) and 2 lime trees (*Tilia Europaea*). Tree parameters like the DBH, total tree height, stem position and tree

species were measured and determined by GPS, tacheometry and the 'Vertex III' system. Furthermore, the trees are subdivided into 3 layers with respect to the top height h_{top} of the plot, where h_{top} is defined as the average height of the 100 highest trees per ha (Heurich, 2006). The lower layer contains all trees below 50% of h_{top}, the intermediate layer refers to all trees between 50% and 80% of h_{top}, and finally, the upper layer contains the rest of the trees. Table 2 summarizes the characteristics of the individual sample plots.

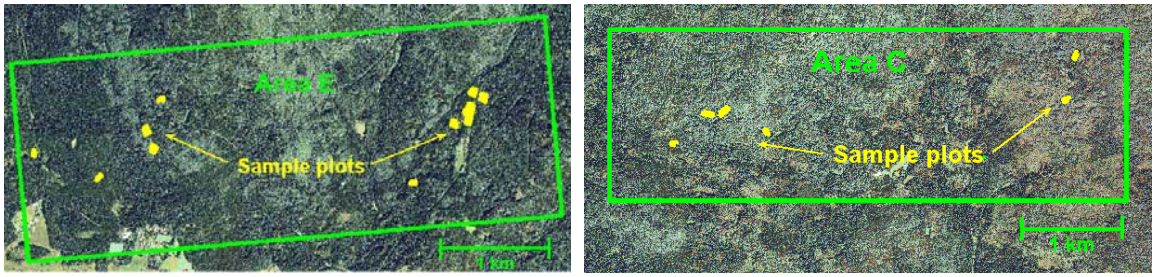

Figure 3: Orthophotos of the test sites E and C and the location of the sample plots

Table 2. Characteristics of sample plots

Plot name	21	22	55	56	57	58	59	60	64	65	74	81	91	92	93	94	95	96
Test site	C	C	E	E	E	E	C	C	C	C	E	E	E	E	E	E	E	E
Age [a]	160	160	240	170	100	85	40	110	100	100	85	70	110	110	110	110	110	110
Size [ha]	0.20	0.20	0.15	0.23	0.10	0.10	0.10	0.10	0.12	0.12	0.30	0.30	0.36	0.25	0.28	0.29	0.25	0.30
Height [m]	860	885	610	640	765	710	810	890	835	875	720	690	764	767	766	768	750	781
N/ha	500	540	830	340	450	440	2150	380	430	810	700	610	260	170	240	250	240	200
N lower layer	37	19	77	31	0	10	76	8	13	53	11	29	31	13	7	15	6	30
N interm. layer	14	60	21	19	4	4	85	22	4	26	33	59	11	3	2	4	0	3
N upper layer	48	29	20	27	41	30	54	27	35	35	165	96	54	27	59	54	53	26
Deciduous [%]	66	79	5	10	0	14	1	100	87	96	29	100	75	100	66	97	10	86

LIDAR data of several ALS campaigns are available for the test sites. First/last pulse data have been recorded by TopoSys with the Falcon II system. Full waveform data have been collected by Milan Flug GmbH with the Riegl LMS-Q560 system. Table 3 contains details about the point density, leaf-on and leaf-off conditions during the flights and the footprint size. The term point density is referring to the nominal value influenced by the PRF, flying height, flying speed and strip overlap. These unique data sets allow the comparison of conventional and full waveform systems, which have been flown in the same area. However, the data set IV is only available for the 12 reference plots in test site E. This has to be considered when comparing results of other data sets with this data set. Naturally, the reference data have been updated for the individual flying dates. Reference trees are plotted in the figures 1a and 1b as black vertical lines.

Table 3: Different ALS campaigns

Time of flight	Sept. '02	May '06	May '07	May '07
Data set	I	II	III	IV
Foliage	Leaf-on	Leaf-off	Leaf-on	Leaf-on
Scanner	TopoSys Falcon II	Riegl LMS-Q560	Riegl LMS-Q560	Riegl LMS-Q560
Pts/m^2	10	25	25	10
HAAT [m]	850	400	400	500
Footprint [cm]	85	20	20	25
Ref. plots	all	all	all	Area E

3.2 Segmentation results

The watershed segmentation ('W') and the new 3D segmentation technique ('Ncut'), using both results from the watershed segmentation and from the stem detection, were applied to all the plots and data sets in a batch procedure without any manual interaction (Table 4). The accuracy and reliability of the presented methods are evaluated in the following way: The tree positions from the segmentation are compared with reference trees if (i) the distance to the reference tree is smaller than 60% of the mean tree distance of the plot and (ii) the height difference between h_{tree} and the height of the reference tree is smaller than 15% of h_{top}. If a reference tree is assigned to more than one tree position, the tree position with the minimum distance to the reference tree is selected. Reference trees that are linked to one tree position are so-called 'detected trees' and reference trees without any link to a tree position are treated as 'non-detected' trees. Finally, a tree position without a link to a reference tree results as a 'false positive' tree.

Table 4: Results of segmentation methods with data sets I, II, III and IV

Data set	Method	Detected trees per height layer [%]				False
		low.	intermed.	up.	total	pos. [%]
I (only area E)	W	2	12	80	52	5
Leaf-on	NCut	15	27	77	55	13
II	W	5	21	77	48	4
Leaf-off	NCut	21	38	87	60	9
III	W	5	20	79	48	4
Leaf-on	NCut	17	32	86	58	10
III (only area E)	W	5	20	82	55	5
Leaf-on	NCut	24	35	88	66	11
IV (only area E)	W	6	21	84	57	6
Leaf-on	NCut	26	33	87	65	11

In the first instance, we want to highlight with data set II how the 3D normalized cut segmentation compares to the 2D watershed segmentation. The 2D segmentation leads to an overall detection rate of 48%, where the detection rate is rather poor in the lower forest layer. The 3D segmentation increases the detection rate considerably in the lower and intermediate layer with about 16%. This is remarkable and shows that the new segmentation technique can successfully detect smaller trees below the CHM. The improvement in the upper layer is 10% and the overall detection rate increases by 12%. The high spatial point density of the full waveform data, which practically contain all relevant reflections of the laser beam, turns out as the key factor to segment in 3D not only the dominant trees but also the dominated smaller trees in the lower and intermediate layers. However, this increased detection rate also deteriorates the reliability of the segmentation process by the factor 2 in terms of false positives. Figure 4 illustrates the improvement of the detection rate graphically.

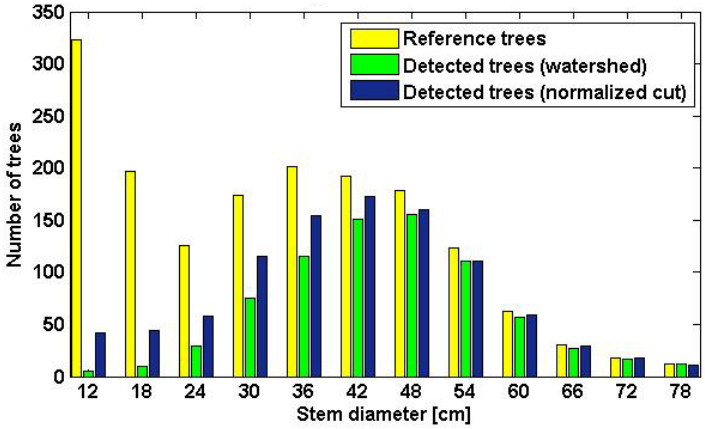

Figure 4: Comparison of single tree detection with data set II

The results given for leaf-off condition (data set II) can also be compared with full waveform data captured in the same area and with the same point density in leaf-on condition (data set III). As expected, the detection rate deteriorates in the case of the normalized cut segmentation in the lower and intermediate layer by roughly 5% due to the reduced penetration rate of the laser beam causing in turn a worse spatial distribution of the reflections. The number of false positives does not change significantly for the normalized cut segmentation.

If we restrict data set III to area E and compare it with data set IV the impact of the nominal point density on the segmentation methods can be analyzed. The comparison of both data sets shows that the detection rate and false positives are practically the same for both point densities. Obviously, although the number of penetrating laser beams is significantly reduced, the most relevant tree structures are still detected by reflections.

Finally, we compare the segmentation methods with respect to first/last pulse data (data set I) and full waveform data (data set IV) that have the same nominal point density. The total detection rate of the 2D watershed based segmentation is by 5% better for the full waveform data. The number of false positives is basically the same. The main reason for this is that the full waveform data represent the tree shape more precisely since the waveform decomposition even detects weak reflections and reflections resulting from adjacent targets. If we focus on the normalized cut segmentation, the benefit of full waveform becomes clearer with an increase of 10%. Most remarkably, the full waveform technique and the normalized cut segmentation outperform the conventional first/last pulse technique and the watershed segmentation by more than 20% in the lower and intermediate layer.

3.3 Classification results

First, we apply an unsupervised and a supervised classification between deciduous and coniferous trees to the 3D segments (Table 5). One fifth of the trees were randomly selected from the entire data set as a training data set for the supervised classification by keeping the proportion between the tree species. Also, both classification methods were applied 20 times in order to minimize the impact of the selection procedure and the initialization of the EM-algorithm of the unsupervised classification on the results. Thus, the numbers in table 5 refer to averaged classification values, whereby the best result of each data set and classification method is highlighted.

Table 5: Results of unsupervised („un.“) and supervised classification („su.“)

Saliency	Overall accuracy (%) for data sets I - IV and for the 2D and 3D segments									
	I (only area E)		II		III		III (only area E)		IV (only area E)	
	un.	su.	un.	su.	un.	su.	un.	su.	un.	su.
S_g^1	80	80	74	75	81	82	83	84	83	83
S_g^2	80	78	75	78	80	82	83	82	81	81
S_i^h	62	66	73	72	64	67	66	66	65	70
S_i^d	66	67	68	76	68	74	69	73	65	70
S_I^1			74	74	90	91	93	93	91	91
S_I^2			81	81	93	94	97	96	95	97
S_W			75	79	52	51	54	56	60	64
S_n^1			80	84	56	54	57	65	66	64
S_n^2			89	93	62	63	61	65	57	57
$S_g^2 + S_I^2$			81	86	90	94	93	97	91	97
$S_g^2 + S_I^2 + S_W + S_n^2$			91	94	81	95	84	97	82	97

If we compare both classification methods with respect to the used saliencies and best results we recognize that in general the supervised classification is slightly better than the unsupervised classification. If we focus on the individual saliencies it is evident that the intensity related saliency S_I^2 turns out as the most important feature in the leaf-on case (data sets III and IV). Data set II proves that the saliency S_n^2 is the best single feature in the leaf-off case. Apparently, coniferous trees cause more single reflections than deciduous trees in leaf-off situation. The saliencies S_i^h and S_i^d describing the penetration of the laser beams in the segmented trees have very little impact on the classification results. The saliency S_W representing the pulse width of the reflections works in general better in the leaf-off case. Finally, the saliencies S_g representing the tree geometry have an almost constant impact on the classification in leaf-on and leaf-off situations. Even for data set I, which refers to first/last pulse data at a point density of 10 pts/m^2, the overall classification accuracy is almost the same as with full waveform data. Thus, this saliency seems to be significant even for the low point density.

The comparison between data set II and data set III indicates that both classification methods are almost the same for both foliage conditions. However, differing saliencies have been used. Furthermore, the results of data set III (only area E) and data set IV (only area E) show also clearly that the point density has practically no influence on the classification results. Thus, the lower point density of 10 pts/m^2 does not appear as disadvantageous. This is consistent with our experience that the segmentation results are also practically the same for both point densities. Finally, the comparison of data set I (only area E) and data set IV (only area E), which both refer to leaf-on situation and a nominal point density of 10 pts/m^2, indicates that the classification with first/last pulse data is significantly inferior by about 15% since only the coordinates of the reflections could be used and hence, the saliencies S_g and S_i could only be calculated for the classification.

The new 3D segmentation provides an interesting insight into the classification accuracy of single trees in different height layers. Table 6 shows how the supervised classification performs in leaf-off (date set II) and leaf-on (data set III) situations. As expected, there is almost no dependency on the height layer in the leaf-off case. Contrary, the classification accuracy deteriorates slightly for the lower and intermediate layers in the leaf-on case. Obviously, the differing classification results are influenced by the lower penetration rate in leaf-on situation.

Table 6: Classification accuracy in dependence on height layers

Data set	Correctly classified trees per height layer [%]			
	lower	intermediate	upper	total
II	95	93	94	94
III	86	90	97	95

Lastly, we want to focus on the question how the tree species spruce and fir can be classified. Table 7 shows the confusion matrix for a supervised classification of 242 spruces and 42 firs, which are located in the sub area E.

Table 7: Confusion matrix of the best classification result for spruces and fir trees

Classified tree species	Spruce	Fir	No. classified segments	User's accuracy
Spruce	230	8	238	97%
Fir	12	34	46	74%
No. reference segments	242	42	284	
Producer's accuracy	95%	81%		
Overall accuracy: 93%	Kappa: 0.72			

We used a combination of the saliencies S_g^2, S_I^2, S_W and S_n^2. The firs, which are proportionally lower represented than spruces, could be classified with 81% accuracy. However, we noticed a standard deviation of 7.7% when we applied the classification procedure 20 times with randomly selected training data sets. We also tried to classify beeches and maples, but failed in any case. Thus, these tree species could not be identified with the data sets and the presented classification procedure.

4. Discussion

The watershed segmentation generates results comparable with results of Heurich (2006), who obtained a detection rate of 45% in almost the same reference areas using also the data set I. Moreover, the experiments prove that the usage of full waveform data is clearly superior to first/last pulse data. The comparison of the different foliage conditions demonstrates a higher detection rate for the leaf-off data set mainly in the lower and intermediate layer because of the higher penetration in unfoliated deciduous trees. Thus, the leaf-off situation seems to be the more appropriate flying time to segment trees in 3D, at least for mixed mountain forests that are scanned with a high point density. The experiment with the different point densities shows that a nominal point density higher than 10 pts/m^2 does not improve the detection rate considerably. However it remains to be seen whether a higher density is advantageous to estimate other parameters like for instance the timber volume. Summarizing, the significant improvement of the detection rate – apparent in the lower and intermediate layer – is influenced both by the full waveform data and the new normalized cut segmentation. The accuracy gain in the lower and intermediate layer is more than 20%.

The classification experiments demonstrate clearly that the overall accuracy is significantly increased by using full waveform data. In general, the accuracy is excellent even for the unsupervised classification. In case of the supervised classification we attained an overall accuracy of 95% for all reference data. Moreover, the results are practically independent on the point density and the foliage condition. Contrary, we have found a slight dependency of the overall accuracy on the height layer in leaf-on situation. However, the accuracy loss is compensated by a superior accuracy in the upper height layer in the leaf-on case. Spruces and firs could be successfully classified as different tree species. Since the number of fir trees was

low further experiments are needed. All in all, the increased detection rate of single trees leads to an increased number of correctly classified trees. For instance, a detection rate of 60% and a classification accuracy of 94% imply 56% correctly detected and classified trees. Finally, our classification results of 80% with first/last pulse data in leaf-on case compare excellent with the experiments of Heurich (2006). However, our results with the full waveform data in leaf-on situation are in any classification case better than the leaf-on results with first/last pulse data of this study.

Acknowledgements

We thank Dr. Marco Heurich and the Administration of the Bavarian Forest National Park for their productive contributions and for giving us the opportunity to use their remote sensing test sites.

References

Brandtberg, T., 2007. Classifying individual tree species under leaf-off and leaf-on conditions using airborne lidar. ISPRS Journal of Photogrammetry and Remote Sensing, 61, pp. 325 – 340.

Heijden, F. van der, Duin, R.P.W., Ridder, D. de and Tax, D.M.J., 2004, Classification, parameter estimation and state estimation – An engineering approach using MATLAB. John Wiley & Sons Ltd, The Attrium, southern Gate, Chichester, West Sussex PO19 8SQ, England

Heurich, M., 2006. Evaluierung und Entwicklung von Methoden zur automatisierten Erfassung von Waldstrukturen aus Daten flugzeuggetragener Fernerkundungssensoren. Forstlicher Forschungsbericht München, Nr. 202, ISBN 3-933506-33-6. http://meadiatum2/ub.tum.de/. (Accessed February 18, 2007).

Holmgren, J., Persson, Å., 2004, Identifying species of individual trees using airborne laser scanner. *Remote Sensing of Environment* 90 (2004) 415 – 423.

Hyyppä, J., Kelle, O., Lehikoinen, M., Inkinen, M., 2001. A segmentation-based method to retrieve stem volume estimates from 3-D tree height models produced by laser scanners. IEEE Transactions on Geoscience and remote Sensing, 39: 969 – 975.

Jutzi, B., Stilla, U., 2006. Range determination with waveform recording laser systems using a Wiener Filter. ISPRS Journal of Photogrammetry and Remote Sensing, 61, pp. 95 – 107.

Kirchhof, M., Jutzi, B., Stilla, U., 2008. Iterative processing of laserscanning data by full waveform analysis. *ISPRS Journal of Photogrammetry and Remote Sensing*, 63, pp. 99 – 114.

Reitberger, J., Krzystek, P., Stilla, U., 2007. Combined tree segmentation and stem detection using full waveform LIDAR data. Proceedings of the ISPRS Workshop Laser Scanning 2007 and SilviLaser 2007,Volume XXXVI, PART 3/W52, 12 – 14th September 2007, Espoo, pp. 332 – 337.

Reitberger, J., Krzystek, P., Stilla, U., 2008a. Analysis of full waveform LIDAR data for the classification of deciduous and coniferous trees. International Journal of Remote Sensing. Vol. 29, No. 5, March 2008 , pp. 1407 – 1431.

Reitberger, J., Schnörr, Cl., Krzystek, P., Stilla, U., 2008b. 3D segmentation of full waveform LIDAR data for single tree detection using normalized cut. *IAPRS* Vol. XXXVII, Part B3a, 3 – 11th July 2008, Beijing, pp. 77 – 83.

Reitberger, J., Schnörr, Cl., Heurich, M., Krzystek, P., Stilla, U., 2008c.Towards 3D mapping of forests: A comparative study with first/last pulse and full waveform LIDAR data. *IAPRS* Vol. XXXVII, Part B8, 3 – 11th July 2008, Beijing, pp. 1397 – 1403.

Shi, J., Malik, J., 2000. Normalized cuts and image segmentation. IEEE Transactions on Pattern Analysis and Machine Intelligence, 22, pp. 888 – 905.

Solberg, S., Naesset, E., Bollandsas, O. M., 2006. Single Tree Segmentation Using Airborne Laser Scanner Data in a Structurally Heterogeneous Spruce Forest. *Photogrammetric Engineering & Remote Sensing,* Vol. 72, No. 12, December 2006, pp. 1369 – 1378.